N93-27564

MAGNETIC GIMBAL PROOF-OF-CONCEPT HARDWARE PERFORMANCE RESULTS

163490

p. 12

Keith O. Stuart
Innovative Information Systems
An Aura Systems Company
Los Angeles, California

1.0 SUMMARY

This report discusses the Magnetic Gimbal Proof-of-Concept Hardware activities, accomplishments, and test results. The Magnetic Gimbal Fabrication and Test (MGFT) program addressed the feasibility of using a magnetic gimbal to isolate an Electro-Optical (EO) sensor from the severe angular vibrations induced during the firing of divert and attitude control system (ACS) thrusters during space flight. The MGFT effort was performed in parallel with the fabrication and testing of a mechanically gimballed, flex pivot based isolation system by the Hughes Aircraft Missile Systems Group. Both servo systems supported identical E-O sensor assembly mockups to facilitate direct comparison of performance. The results obtained from the MGFT effort indicate that the magnetic gimbal exhibits the ability to provide significant performance advantages over alternative mechanically gimballed techniques.

2.0 INTRODUCTION

The MGFT effort was funded by the U. S. Air Force under the SDI KEW Program, formally known as the Kinetic Kill Vehicle (KKV) Program. The hardware proof-of-concept study was conducted from March to November, 1986.

The specifications imposed on the magnetic gimbal required the angular vibrations transmitted to the E-O sensor's optical path be less than 100 microradians, even during 10 g lateral divert maneuvers. A series of environmental tests were to be conducted at the Hughes MSG facility where the performance of the magnetic suspension system was to be evaluated. These tests included mounting of the MGFT hardware onto shaker tables and measuring the E-O sensor mockup's line-of-sight (LOS) while specific vibration profiles were produced.

A parallel effort involving the flex pivot gimbal fabrication and test was performed and this system was subjected to similar specifications and evaluations.

A detailed structural analysis of the E-O sensor mockup was provided to the control system engineers responsible for the two efforts to aid in the design of the respective servo systems.

2.1 DESCRIPTION OF MGFT HARDWARE AND SOFTWARE

Figure 2.1 shows the completed MGFT hardware. Hardware components that were designed, fabricated or procured, and integrated into the system are listed below.

1. Dual magnetic bearings (see figure 2-2 for a photograph of one of the bearings during characterization testing)
2. Bearing support fixtures
3. Rotary actuator
4. Automatic autocollimator (for LOS servo position feedback)
5. E-O Sensor assembly structural mockup
6. Custom 5-channel digital servo processing board based on a Motorola 68020 Microprocessor and 12 bit A/D and D/A convertors.

These items represent the necessary components involved in the various servo loops that control the magnetic suspension and line-of-sight of the E-O sensor mockup.

The magnetic bearings, one of which is shown in figure 2-2, were designed to utilize Simarian Cobalt (SmCo) permanet magnets to linearize the relationship between coil current and force exerted across the gap. Figure 2-3 shows a layout of the bearing used for the MGFT Program.

The bearing support fixtures were designed for structural rigidity. No size requirements were imposed.

The automatic autocollimator provided a highly accurate analog angular position reference to the E-O sensor LOS servo.

The E-O sensor mockup was provided to IIS by Hughes and was outfitted with optical quality mirrors used during the measurement of vibration rejection and for closure of the LOS position servo.

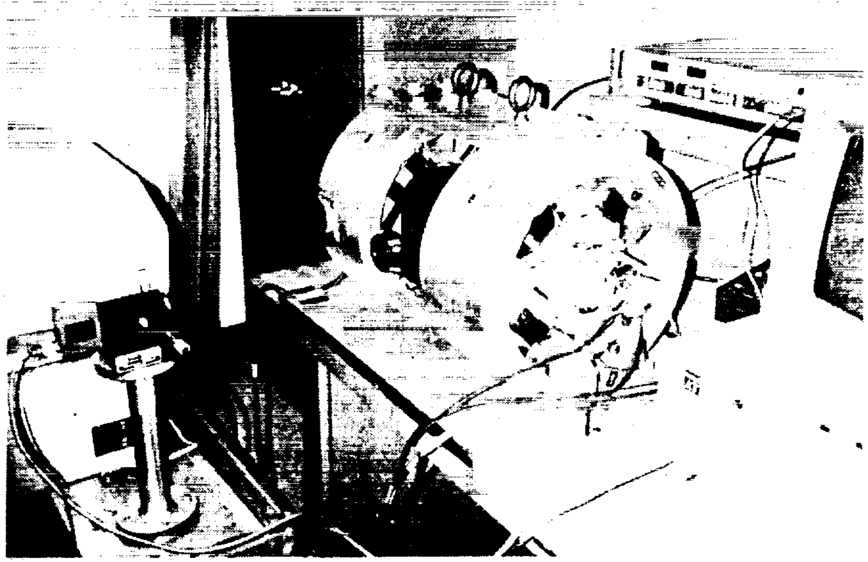

FIGURE 2-1. MAGNETIC SUSPENSION AND POINTING SYSTEM DEVELOPMENT FOR PHASE 1 RISK REDUCTION EFFORT

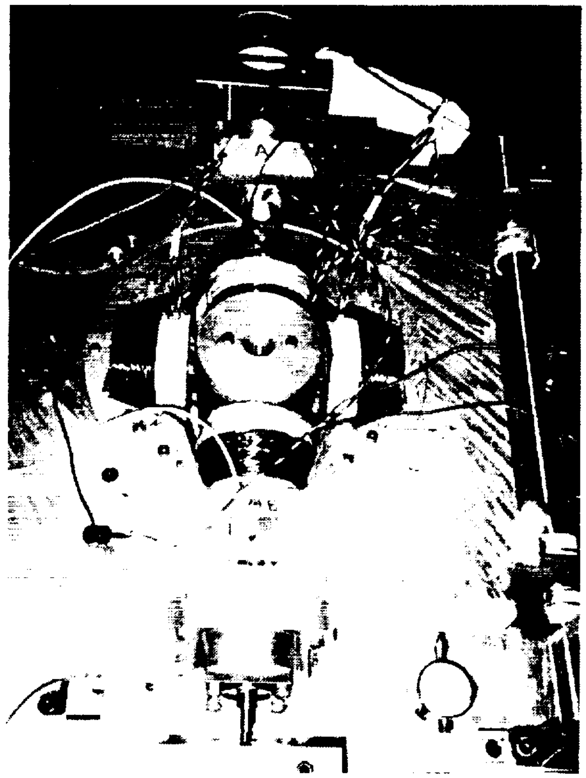

FIGURE 2-2. MAGNETIC BEARING IN TEST FIXTURE

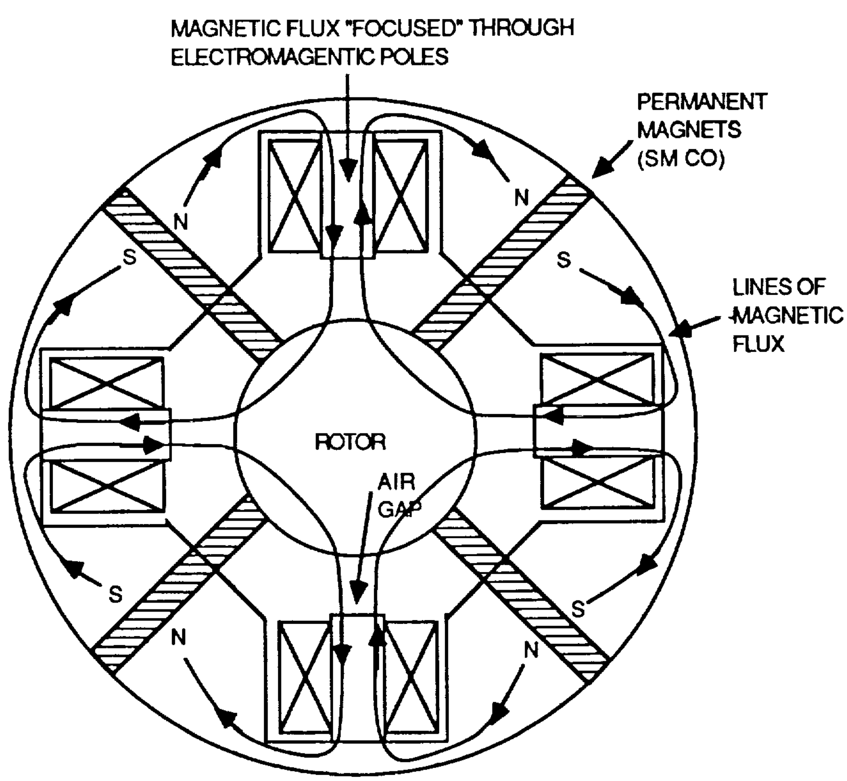

FIGURE 2-3. MAGNETIC CIRCUIT USED FOR PAYLOAD EXPERIMENT

The following digital servo systems were implemented in software on the 68020 and developed for the MGFT Program during the months of May to September, 1986.

a. Four digital magnetic suspension servos
b. One digital pointing control servo (LOS servo)
c. One digital acceleration feedforward compensator

The digital servo algorithms are serviced serially by the 68020 to provide the magnetic suspension and control the angular position of the seeker structural model.

The digital servo processing board is mounted in an IBM PC/AT compatible computer for ease of program development and downloading, and to allow real-time monitoring and modification of servo parameters. A real-time servo monitor and modification program was developed, allowing the controls engineer to observe and modify important servo parameters during operation. This interactive servo parameter modification software drastically reduces the time required for servo performance optimization. This technique is applicable to automated servo optimization, where a host computer can vary servo parameters to achieve specific performance requirements via a pre-determined rule-based algorithm.

3.0 SUMMARY OF TEST RESULTS

The vibration testing to be preformed for the MGFT Program followed as closely as possible the testing done for the flex pivot gimbal system. Two vibration tests were performed: torsional vibrations and linear vibrations. Figure 3-1 shows how each type of motion was induced.

The objective of the test sequences was to infer the line-of-sight stability of the KKV seeker assembly during the terminal portion of flight. This objective was met by disturbance definition, seeker geometry, test set-up and procedure and the vibration isolation system. Hughes Missile System group provided the first 3 items, and IIS provided the last item.

Each test involved the measurement of the level of motion disturbance which passed through to the isolated gimbal system due to a predefined vibration disturbance induced by a shaker table. Both shaker table vibration and the vibration motion transmitted to the seeker assembly was measured with optical measurement equipment (Optrons and Autocollimators). The data from these devices was recorded by a Hewlett Packard frequency analyser. All testing was done in the Hughes Missile System Group's Vibration Lab located in Canoga Park, California. The vibration testing was done on a Unholtz-Dickie model 1000 shaker table controlled with a Hewlett Packard computer system. The optical sensing equipment was placed on an air-bag table next to the shaker table to isolate them from unwanted vibrations. A photograph of the torsion table set-up can be found in figure 3-2.

Both torsional and lateral test sequences were performed. The following sections summarize the results of those test sequences.

3.1 TORSIONAL VIBRATION TESTING

A diagram of the torsional test set-up can be found in figure 3-3. A total of 4 different tests were performed: Simulated Thruster Pulses test, Amplitude Sweep, Frequency Sweep, and Lateral Suspension Stiffness test.

3.1.1 Simulated Thruster Pulses Test

The Simulated Thruster Pulses test examined the gimbal's ability to isolate motion waveforms representing realistic worst-case torsional disturbances produced by the firing of the missile's divert and ACS thrusters. These motion waveforms were provided by Hughes Aircraft Missile Systems Group.

A total of 4 different torsional waveshapes were tested. Each of these disturbance waveshapes had a fundamental frequency of 10 Hz. In each of the four pulses tested, the gain of the pointing control servo was reduced gradually until completely eliminated, allowing the suspended sensor's own inertia to stabilize it's LOS. This is only possible due to the frictionless nature of the magnetic suspension, since no mechanical coupling occurs between the sensor and the outside world. The reduction of the pointing servo gain had the effect of reducing the servo's closed loop bandwidth, an effect verified during the frequency-analysis phase of the servo development.

Figure 3-4 contains the reduced data for each of the four torsional pulse shapes. In summary, the level of vibration isolation between the high pointing servo bandwidth case (60 Hz closed loop bandwidth) and no pointing servo is very close, yielding rejection ratios from -50 dB to -60 dB depending on the waveshape. When the pointing servo bandwidth approached the disturbance waveform's fundamental frequency, a peaking of the transmitted disturbance resulted. This resonance phenomena can be explained by the increase of the closed loop servo gain (gain overshoot) just prior to roll-off.

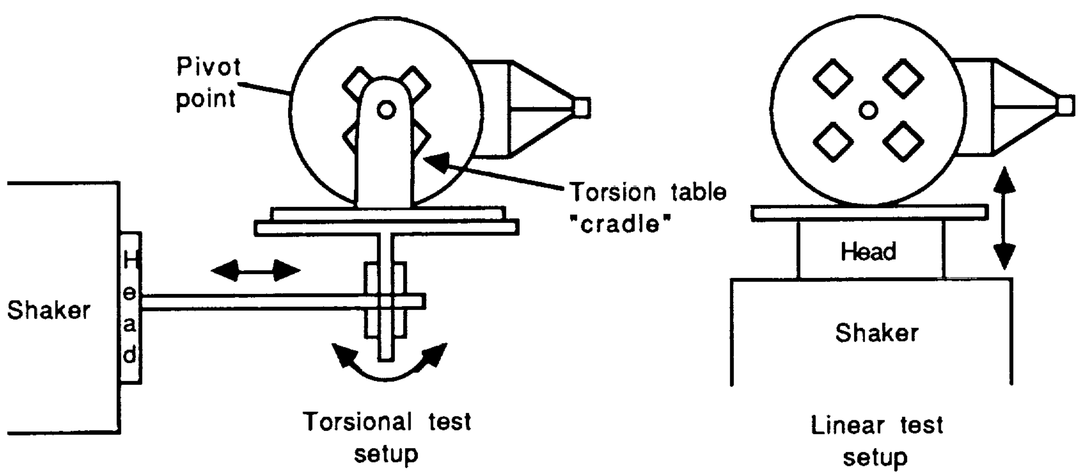

FIGURE 3-1. MECHANICAL METHODS OF INDUCING VIBRATIONAL DISTURBANCES

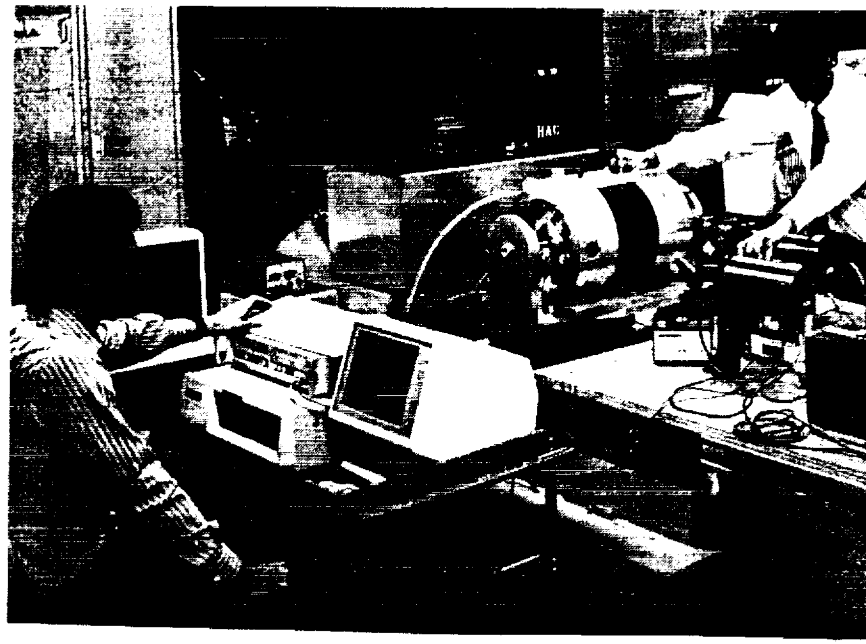

FIGURE 3-2. PAYLOAD EXPERIMENT TEST SETUP AT HUGHES VIBRATION LABORATORY

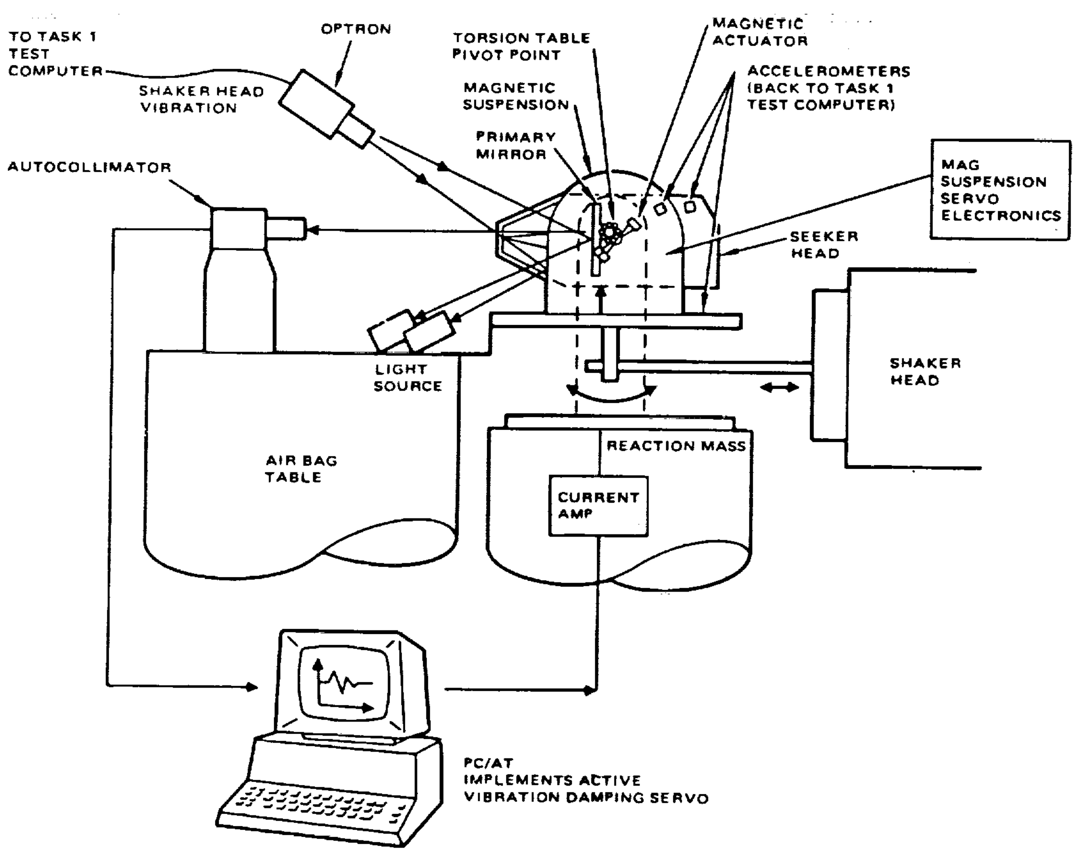

FIGURE 3-3. TORSIONAL TEST SET

CONTROL SERVO BANDWIDTH, Hz	DISTURBANCE AMPLITUDE, MILLIRAD	TRANSMITTED ANGULAR VIBRATIONS, μrad	REJECTION RATIO	
			ABSOLUTE	DB
60*	3.9	4.1	956.0	59.6
60*	3.9	3.1	1247.0	61.9
60*	3.9	5.0	775.2	57.8
45	3.9	6.9	564.8	55.0
23	3.9	13.6	286.8	49.2
12	3.9	10.9	358.5	51.1
0	3.9	5.1	764.8	57.7

*GAIN VARIED FOR FIRST 3 CASES. SEE APPENDIX A

a) Pulse 1
FIGURE 3-4. TORSIONAL TEST

CONTROL SERVO BANDWIDTH, Hz	DISTURBANCE AMPLITUDE, MILLIRAD	TRANSMITTED ANGULAR VIBRATIONS, μrad	REJECTION RATIO	
			ABSOLUTE	DB
60	5.6	5.2	1082.6	60.6
60	5.6	7.02	801.9	58.1
60	5.6	12.7	441.0	52.9
45	5.6	17.7	318.0	50.0
23	5.6	18.3	306.3	49.7
12	5.6	18.3	306.3	49.7
0	5.6	6.1	918.8	59.2

b) Pulse 2
FIGURE 3-4B TORSIONAL TEST RESULTS

POINTING SERVO BANDWIDTH, Hz	DISTURBANCE BANDWIDTH, Hz	TRANSMITTED ANGULAR VIBRATIONS, μrad	REJECTION RATIO	
			ABSOLUTE	DB
60	3.5	4.2	838.6	58.5
60	3.5	4.5	787.8	57.9
60	3.5	4.7	742.8	57.4
45	3.5	5.1	694.1	56.8
23	3.5	10.2	346.6	50.8
12	3.5	8.8	400.0	52.0
0	3.5	6.4	554.6	54.8

c) Pulse 3
FIGURE 3-4. TORSIONAL TEST RESULTS

POINTING SERVO BANDWIDTH, Hz	DISTURBANCE AMPLITUDE, MILLIRAD	TRANSMITTED ANGULAR VIBRATIONS, μrad	REJECTION RATIO	
			ABSOLUTE	DB
60	3.2	5.6	571.9	55.1
60	3.2	6.2	516.2	54.3
60	3.2	9.9	325.3	50.2
45	3.2	15.7	204.0	46.3
23	3.2	15.3	209.6	46.4
12	3.2	13.6	267.8	48.5
0	3.2	7.8	410.2	52.3

d) Pulse 4
FIGURE 3-4. TORSIONAL TEST RESULTS

The amount of vibration transmitted to the seeker when the pointing servo overshoot frequency was away from the primary vibrational resonance frequency varied between 4.2 microradians to 7.8 microradians peak-to-peak, which averages about a factor of 20 below the 100 microradian specification limit. The resonance frequency vibrations climbed as high as 15.7 microradians peak-to- peak, or about a factor of 6 below the spec limit.

Figure 3-5 shows a comparison of the angular vibration isolation test results of the flex pivot gimbal and the IIS magnetic gimbal. The upper graph shows the transmitted vibration of both the magnetic gimbal and flex pivot with the same input disturbance, shown in the lower graph. The peak-to-peak vibration transmitted to the seeker with the flex pivot is 125 microradians, giving a rejection ratio of -35 dB. The peak-to-peak vibrations transmitted through the magnetic suspension for the same disturbance input is 5.2 microradians, achieving a rejection ratio of -60.6 dB.

3.1.2 Amplitude Sweep Test

The amplitude sweep test was performed to study the correlation between input disturbance amplitude and disturbance transmitted through the magnetic gimbal. The amplitude of a 10 Hz sinusoidal angular motion was increased from 10 milliradians peak-to-peak to over 77 milliradians peak-to-peak. The results of the test is shown in figure 3-6.

With an amplitude disturbance of 10.0 milliradians, the amount of transmitted vibration was 5.1 microradians (-65.8 dB rejection). An amplitude of 77 milliradians produced a transmitted vibration of 8.5 microradians (-79.1 db rejection). The conclusion reached was that the amount of vibration transmitted through the magnetic suspension system is essentially independent of the amplitude of the disturbance.

3.1.3 Frequency Sweep Test

The frequency sweep test was performed to study the correlation between input disturbance frequency and disturbance transmitted through the magnetic gimbal. The frequency of a sinusoidal angular motion disturbance with a constant input angular acceleration of 48 rad/sec^2 was increased from 10 Hz to 200 Hz. The results of the test is shown in figure 3-7.

The amount of vibration transmitted over the 10 Hz to 200 Hz frequency sweep varied from 5.3 microradians (at 200 Hz) to 12.7 microradians (at 20 Hz). This increase at 20 Hz corresponded to the pointing control servo overshoot frequency of 30 Hz. The conclusion reached from this test is that the amount of transmitted vibration is independent of disturbance frequency except around the pointing servo overshoot frequency. This problem can be solved by designing the pointing servos to place the overshoot frequency far away from the thrusters primary pulse frequency.

3.1.4 Lateral Suspension Stiffness Test

The lateral suspension stiffness test was performed to study the correlation between the closed-loop bandwidth of the digital suspension servo (which is a function of the "stiffness" of the magnetic bearings) and the disturbance transmitted through the magnetic gimbal. The closed loop bandwidth of the suspension servos were modified by increasing the servo gain from a point where it was almost unstable due to lack of gain to the point where it was almost unstable due to too much gain. As with the pointing servo, the effect of the variation of gain on the closed loop bandwidth was verified during the frequency analysis portion of the servo development.

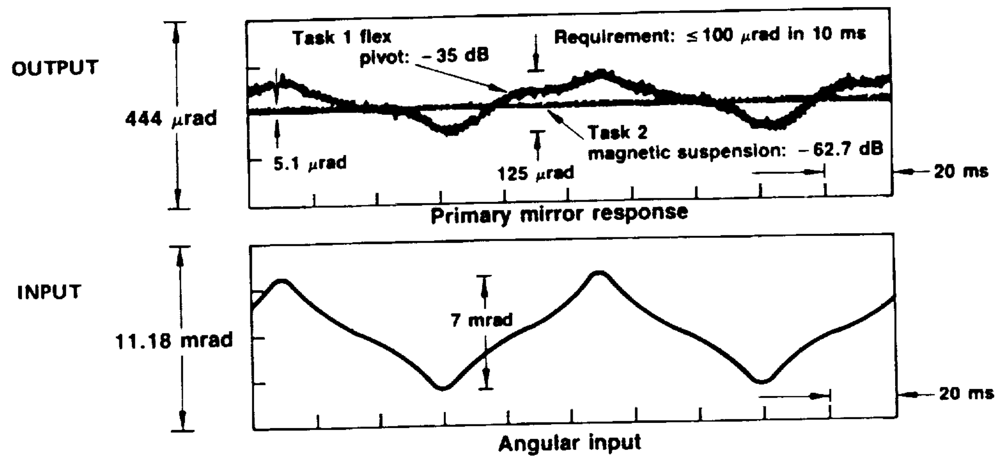

FIGURE 3-5. ANGUALAR VIBRATION ISLOATION TEST RESULTS FOR TASK 1 FLEX PIVOT AND TASK 2 MAGNETIC SUSPENSION SYSTEM

INPUT ANGULAR ACCELERATION, rad/sec^2	BULKHEAD DISTURBANCE AMPLITUDE, MILLIRAD, PEAK-TO-PEAK	TRANSMITTED ANGULAR VIBRATIONS, μrad PEAK-TO-PEAK	REJECTION RATIO	
			ABSOLUTE	DB
16	10.0	5.1	1958.3	65.8
32	20.5	6.5	3092.2	69.8
48	28.2	7.4	3786.8	71.5
64	40.5	8.5	4758.8	73.5
80	~56	7.7	7311.1	77.3
96	~72	8.8	8134.6	78.2
112*	~77	8.5	9047.5	79.1

*LIMIT OF SHAKER TABLE

FIGURE 3-6. TORSIONAL AMPLITUDE SWEEP TEST RESULTS

INPUT FREQUENCY, Hz	BULKHEAD (DISTURBANCE) AMPLITUDE, MILLIRAD, PEAK-TO-PEAK	TRANSMITTED ANGULAR VIBRATIONS, μrad PEAK-TO-PEAK	REJECTION RATIO	
			ABSOLUTE	DB
10	24.3	7.4	3263.1	70.3
20	8.01	12.7	627.4	55.9
50	1.09	6.8	160.8	44.1
100	0.735	7.9	92.1	39.3
200	0.106	5.3	5.0	26.0

FIGURE 3-7. TORSIONAL FREQUENCY SWEEP TEST RESULTS

The servo bandwidth was varied from a minimum of 82 Hz to a maximum of 120 Hz. A constant sinusoidal disturbance with a frequency of 10 Hz and an amplitude of 28.2 milliradians was applied. The results of the test is shown in figure 3-7. The angular vibrations transmitted to the seeker varied randomly from 6.0 microradians to 8.1 microradians. The conclusion reached from this test is that the amount of transmitted vibration is independent of lateral suspension stiffness.

3.2 LATERAL TESTS

The purpose of the lateral tests was to test the ability of the magnetic gimbal to remain operational during a severe lateral disturbance. As shown in figure 3-1, the magnetic gimbal assembly was placed directly on top of the shaker table.

As illustrated in figure 3-8, due to the extremely fast rise time of the simulated lateral thruster pulses (0 to maximum acceleration in less than 3 msec, and a maximum acceleration of 10 G's), the suspension servo alone could not handle pulses greater than approximately 0.8 G's. Above that amount, the shaft would strike its mechanical stop.

To improve this situation, acceleration feedforward compensation was added to the suspension control system that increased the effective bandwidth of the suspension servos from approximately 100 Hz to 500 Hz. With the compensation servo, the system could handle pulses of up to approximately 3 G's. Above 3 G's, the weight of the seeker structural model (16.5 lbs. total) and the high inductance of the magnetic bearing coils (.021 henries) became the limiting factors. The voltage amplifier saturated because of the high voltage levels required to overcome the coil inductance during the 3 msec disturbance pulse rise time.

The design modifications required to handle high lateral level, fast rise time accelerations are straightforward, low risk and utilize existing technology. They include increasing the effective speed of the suspension servo CPU's by a factor of 5 (accomplished by using a high speed digital signal processor to service all 5 servo systems or use a dedicated processor for each servo channel), incorporate acceleration feedforward compensation, design the magnetic suspension system to minimize electromagnetic coil inductance and increase the voltage headroom of the power driving system to overcome the remaining inductance. These modifications have been successfully implemented in subsequent systems.

SUSPENSION SERVO BANDWIDTH, Hz	TRANSMITTED ANGULAR VIBRATIONS, μrad PEAK-TO-PEAK	REJECTION RATIO	
		ABSOLUTE	DB
82	6.0	4883.3	73.8
91	8.0	3662.5	71.3
98	7.4	3934.6	71.9
105	6.9	4237.2	72.5
110	6.8	4303.4	72.7
120	8.1	3586.2	71.1

FIGURE 3-8. TORSIONAL SUSPENSION STIFFNESS TEST RESULTS

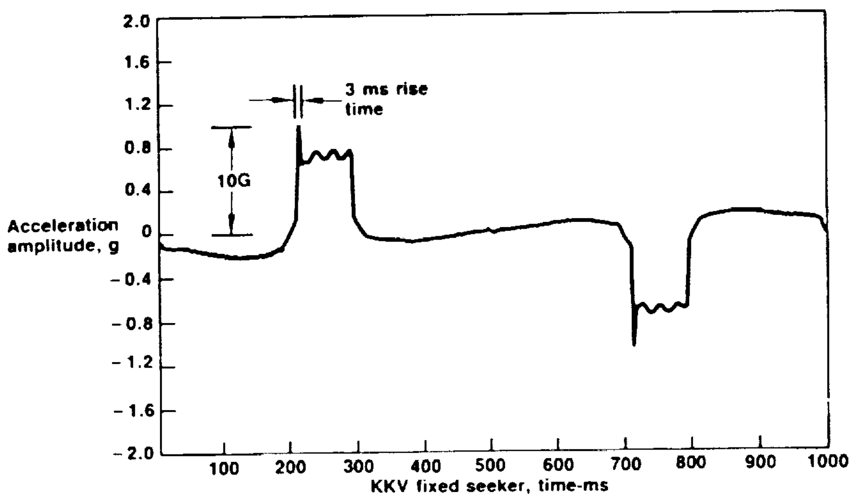

FIGURE 3-9. THRUSTER LATERAL PULSE WAVEFORM

4.0 CONCLUSIONS

Results from the the MGFT Program effort show that the magnetic suspension and pointing technology developed by IIS is highly suited for the gimballing requirements of systems requiring an extremely high degree of pointing accuracy in a severe vibrational environment. This effort also proved that digital magnetic suspension servos can be implemented quickly, reliably and inexpensively using commercially available hardware components.

The specific results and conclusions derived from the the MGFT Program for the Kinetic Kill Vehicle Weapon System indicate that magnetic suspension and pointing control will provide the following benefits when compared to alternative mechanically supported systems:

- Vastly superior angular vibration isolation due to the elimination of physical contact of the seeker with the interceptor's bulkhead (20 times better than spec)

- Elimination of the need for super-precise and repeatable machining (such as is required on high-accuracy pre-loaded ball bearing gimbal systems or flex pivot manufacturing)

- Ability to increase lateral stiffness of the gimbal without effecting its torsional stiffness

- Ability to automatically custom-tune the compliance of each individual gimbaled seeker system during assembly to relax required manufacturing tolerances

- High reliability and longevity in the space environment

The benefits of magnetic suspension and pointing control make this system a low cost, highly reliable and super-preforming gimbal that should be considered for use in any high precision pointing application.